Optimum Treatment Time for Solid-State Extraction of Nickel from Nickel Sulfide Concentrates at 1073 K

FANMAO WANG, SAM MARCUSON, LEILI TAFAGHODI KHAJAVI, and MANSOOR BARATI

Solid-state thermal treatment of Ni sulfide concentrates in an inert or reducing atmosphere, and the presence of metallic Fe is proposed as a feasible route to produce ferronickel (FeNi) alloy while retaining S in iron sulfides. The present work investigated the effects of temperature and amount of Fe addition *via* a thermodynamic analysis, giving a suitable temperature of 973 K to 1173 K and metallic Fe to Ni concentrates mass ratio of 0.5 to 2. The minimum time required for Ni extraction at 1073 K was investigated *via* thermal treatment experiments of various durations, and it was determined to be 30 minutes. Under the tested experimental conditions, average Ni concentration in the resulting sulfides and the generated FeNi was found to be 0.5 ± 0.2 mass pct and 16 to 18 mass pct, respectively, and in good agreement with the thermodynamic predictions. The maximum Ni recovery to FeNi was approximately 97 pct and the characteristic particle sizes d_{10} and d_{80} of FeNi were 14 and 45 μm, respectively. During 360 minutes of the thermal treatment, only 0.7 mass pct of S in the concentrates was released to the off gas as SO_2.

https://doi.org/10.1007/s11663-020-01960-3

I. INTRODUCTION

NICKEL is a critical alloying element in steels,[1,2] other corrosion-resistant alloys,[3] and batteries.[4] Approximately, 60 pct of the annual Ni production worldwide is consumed in the stainless steel industry.[5,6] The conventional route to extract Ni from Ni sulfide concentrates involves smelting and refining to remove the Fe and S associated with Ni. During smelting, sulfur in the concentrate is oxidized to SO_2 and reports to the off gas, while Fe is oxidized to FeO and is slagged off. When SO_2 concentration in the off gas is 10 to 12 vol pct, it can be effectively captured for sulfuric acid production,[7] while more dilute gases are often vented to the atmosphere. Sulfur dioxide mitigation in Ni smelters constitutes significant operating and capital costs, sometimes greater than the smelting cost itself. Further, there are considerable environmental hazards and penalties associated with any SO_2 emitted to the atmosphere. As a result, handling SO_2 emissions from the smelter remains a challenge or a cost driver for the Ni industry.

Through laboratory experiments, the concepts of selective oxidation-sulfation or oxidation-chlorination roasting followed by water leaching has been proposed as an alternative route for the conventional smelting process.[8–12] Yu *et al.* reported that oxidation-sulfation of nickel sulfide concentrate at 973 K for 150 minutes, with the addition of 10 mass pct Na_2SO_4 results in recovering 79, 91, and 95 pct of Ni, Cu, and Co, respectively.[11,12] Mu *et al.* found that under the optimum conditions of temperature (448 K), $FeCl_3{\cdot}H_2O$ addition (50 mass pct), and time (120 minutes), the maximum recoveries of Ni and Cu were 92 and 89 pct after water leaching.[9] These alternate processes have to separate Ni and Cu from the leach solution, adding an electro-winning step to the process flowsheet. Furthermore, SO_2 and SO_3 gases are still generated during the roasting step, and effluent treatment is a must.

The presence of oxygen either in the conventional smelting or the aforementioned selective roasting inevitably leads to the generation of SO_2. The concept of an oxygen-free thermal treatment process for the recovery of Ni from pyrrhotite tailings was put forward and tested by Sridhar *et al.*[13] In this method, the Fe/S ratio of the sulfide is increased by adding Fe or removing S, leading to precipitation of ferronickel (FeNi). Recently, this method was further developed by Liu *et al.*[14] and Yu *et al.*[15]; they confirmed that in

FANMAO WANG, SAM MARCUSON, and MANSOOR BARATI are with the Department of Materials Science and Engineering, University of Toronto, 184 College Street, Toronto, Ontario M5S 3E4, Canada. LEILI TAFAGHODI KHAJAVI is with the Department of Materials Engineering, University of British Columbia, 309-6350 Stores Road, Vancouver, British Columbia V6T 1Z4, Canada. Contact e-mail: fanmao.wang@mail.utoronto.ca

Manuscript submitted on May 28, 2020.
Article published online September 23, 2020.

the presence of metallic Fe and under inert or reducing atmosphere, S in pyrrhotite is trapped by Fe and FeNi is produced.

Since Ni sulfide concentrate is essentially a Fe-Ni-S system, this non-oxidizing thermal treatment is expected to suppress the evolution of SO_2 while extracting Ni in the form of FeNi. This concept was validated in our previous work.[16] It was found that thermal processing of Ni sulfide concentrates at 1223 K in an inert atmosphere and in the presence of Fe, results in Ni extraction as FeNi alloy while retaining the bulk of S as solid FeS. This solid-state extraction is intended to provide an SO_2-free avenue for Ni extraction. Also, Ni grade in the produced FeNi was ~ 22 mass pct, providing a potential source of Fe and Ni for stainless steel.[17] However, the maximum Ni recovery to FeNi at 1223 K was lower than 80 pct. Furthermore, the optimum operating temperature, amount of Fe addition, and the heating time for this solid-state extraction are required. In the present work, thermodynamic assessment is employed to investigate the effects of temperature and the amount of Fe addition. The optimum heating time is determined by high temperature experiments.

II. MATERIALS AND METHODS

A. *Materials*

The composition of a commercial Ni sulfide concentrate is listed in Table I. As seen, the concentration of Ni is 18.8 mass pct, and the primary Ni-bearing mineral is $Fe_{4.5}Ni_{4.5}S_8$ (Pentlandite, Pn) that accounts for ~ 56 mass pct of the concentrates. Furthermore, the characterized particle size of the Ni sulfide concentrate is d_{80} = 30 μm.

B. *Methods*

1. *Thermodynamic evaluation*

FactSage ™ 6.4 was employed to conduct the equilibrium calculations.[18] The selected database and the calculation method were described in a previous study.[16] When performing the evaluation, 100 weight units of the normalized Ni-Cu-Co-Fe-S was chosen as a basis: Ni 23.3, Cu 1.9, Co 0.4, Fe 37.3, and S 37.1 weight units. Various amounts of metallic Fe were added to the system to investigate phase evolution and Ni distribution in these phases. The amount of Fe addition is described as the mass ratio of metallic Fe to Ni concentrates, denoted by m.

2. *Thermal treatment tests*

A schematic of the experimental apparatus is presented in Figure 1. For each experiment, 10 g of Ni concentrate was thoroughly blended with 12 g of metallic Fe with > 99 pct purity. Then the mixture of the concentrate and Fe was pressed into 16 mm D×12 mm H briquettes. Prior to thermal treatment, the briquettes were placed on an alumina holder and retained in the cold zone of the furnace tube. Once furnace temperature reached 1073 K, the holder containing the briquettes was quickly pushed to the hot zone and kept there for various times from 5 to 360 minutes, as detailed in Table II.

To preserve the equilibrium conditions achieved at 1073 K, the holder was transferred to the cold zone, where the temperature was below 423 K. For an effective quenching, an alumina column was placed in front of the holder to reduce the radiative heat transfer to the cold zone. Ar (> 99.9 pct purity) was purged throughout the experiments at a rate of 400 mL/minutes.

3. *Analysis of thermal treatment products*

Scanning electron microscopy (SEM) and electron probe micro-analysis (EPMA) were employed to examine the morphology and compositions of the products. Image analysis using ImageJ was conducted to investigate the FeNi particle size. An infrared continuous gas analyzer (EL3020, ABB) was employed to detect the concentration of the evolved SO_2 in the off gas during thermal treatment. The phase changes before and after thermal treatment were examined by X-ray diffraction (XRD).

III. RESULTS AND DISCUSSION

A. *Thermodynamic Evaluation*

The fundamental support for this solid-state extraction relies on the thermodynamics of Fe-Ni-S system where Fe can substitute for Ni in the Fe-Ni-S system and precipitate FeNi from the matrix.[13–16] The Fe-Ni-S phase diagram is employed to describe the phase evolution with Fe addition. As shown in Figure 2, for example, at 973 K, the initial concentrate lies in a pyrrhotite (Pyrr) phase region, a Ni-rich monosulfide. Adding Fe to the concentrate while fixing the S/Ni shifts the equilibrium toward the Fe corner (along the dotted arrow), first passing a Beta-Ni_3S_2 – Pyrr region and then reaching the FeNi (fcc)-Pyrr domain. As a result, FeNi (fcc) is generated and S is retained as solid Pyrr.

The phase constitution in the system is affected by temperature and the overall composition. Figure 3 illustrates the proportions of various phases at different temperatures as a function of Fe addition. Below 1123 K, the equilibrium mainly consists of FeNi, solid sulfide, and β-Ni_3S_2. The liquid phase starts to form at 1073 K. Increasing temperature results in a higher amount of liquid. On the other hand, for a fixed temperature, with increasing m, the amount of FeNi is

Table I. Chemical and Mineralogical Composition of Ni Sulfide Concentrate

Element	Concentration[a] (Mass Pct)	Normalized Concentration[b] (Mass Pct)	Estimated Mineralogy	Content[c] (Mass Pct)
Ni	18.8	23.3	$Fe_{4.5}Ni_{4.5}S_8$	56
Cu	1.6	1.9	$CuFeS_2$	5
Co	0.3	0.4	$Fe_{4.5}Co_{4.5}S_8$	1
Fe	30.1	37.3	Fe_7S_8 + FeS_2	21
S	29.9	37.1	Silica	8
C	3.8		Rock	9
Si	2.4			
O	9.7			
Other	3.4			
Total	100	100	Total	100

[a]Elemental concentration in the sulfide concentrate.
[b]Normalized concentration of Ni, Cu, Co, Fe, and S in the five sulfides.
[c]Estimated mass percentage of various minerals in the concentrate.

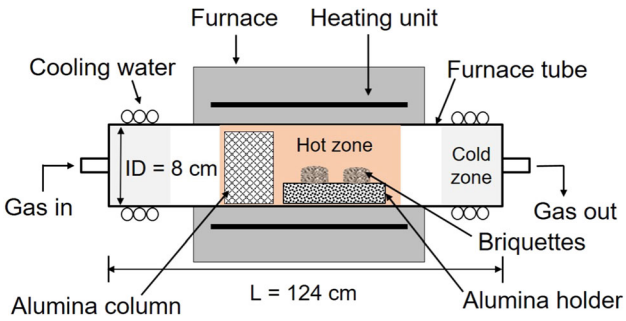

Fig. 1—Schematic of the thermal treatment setup.

increased. Note that at 973 K two structures of FeNi exist, *i.e.*, fcc and bcc; above 973 K the FeNi is present only with an fcc structure.

The theoretical grade (*i.e.*, pct Ni in the alloy) and recovery of Ni in the FeNi were calculated from the phase constitution and composition of each phase. The effect of Fe addition and temperature on Ni grade and recovery are shown in Figure 4. In the range 973 to 1123 K, Ni recovery increases dramatically to over 90 pct when m approaches 0.5 (Figure 4(a)). This is because the equilibrium shifts to a FeNi-containing phase region at $m = 0.5$ (Figure 3). The recovery levels off by increasing m beyond 0.5. At 1223 K and 1273 K, however, the recovery is much lower than that at 973 K to 1173 K for a given m. It is also evident that temperature has a negative effect on Ni grade in FeNi: the higher the temperature, the lower the Ni grade. The maximum achievable grade is ~ 60 mass pct at 973 K; however, at 1273 K the maximum grade is ~ 20 mass pct. Because metallic Fe dilutes the FeNi, surplus Fe lowers the Ni grade. When m is between 0.25 and 0.5, the Ni grade has the highest value, and then it decreases with m.

The adverse effect of high temperature on Ni extraction can be explained using Figure 5. Taking $m = 1.2$, 34 and 41 mass pct of Ni is distributed in liquid at 1223 K and 1273 K, resulting in a small mass fraction of Ni in FeNi. Therefore, as shown in Figure 4(a), the maximum Ni recovery to FeNi at 1223 K and 1273 K is smaller than Ni recovery at lower temperatures.

The goal of this work is to produce a FeNi with > 10 mass pct Ni, a comparable grade to the current marketable FeNi[19,20] and a reasonable grade for the stainless steel production.[17] Considering both grade and recovery, the suitable operating temperature is chosen as 973 to 1173 K, and the appropriate amount of Fe addition (m) is selected to be in the range of 0.5 to 2. Under these conditions, the maximum theoretical recovery of Ni to FeNi is 94 to 98 pct, with the Ni grade in the range of 10 to 36 mass pct. The present work employs the operating temperature of 1073 K and $m = 1.2$ for experimental investigation. The Ni recovery and grade under these conditions are predicted to be 98 pct and 16 mass pct, respectively.

B. *Micromorphology*

Figure 6 shows the microstructure of the product treated at 1073 K for 240 minutes; after thermal treatment, Ni mostly coexists with Fe rather than S. This demonstrates that the thermal treatment redistributes Fe, Ni, and S toward the formation of a Ni-rich FeNi alloy and a Ni-lean sulfidic phase. Furthermore, the mapping of Ni shows two types of FeNi with distinct Ni grade: FeNi1 with low Ni content and FeNi2 with high Ni content. As seen, FeNi1 has a large particle size; FeNi2 particles are smaller in size and located in the sulfide matrix.

Table II. Experimental Conditions for Ni Extraction

Test No.	Heating Time (Minutes)	Temperature (K)	m[a]	Mass of Ni Concentrate (g)	Mass of Metallic Fe (g)	Fe Particle Size, d_{100} (μm)
1	5	1073	1.2	10	12	74
2	10					
3	30					
4	60					
5	120					
6	240					
7	360					

[a]m is the mass ratio of Fe addition to Ni sulfide concentrate.

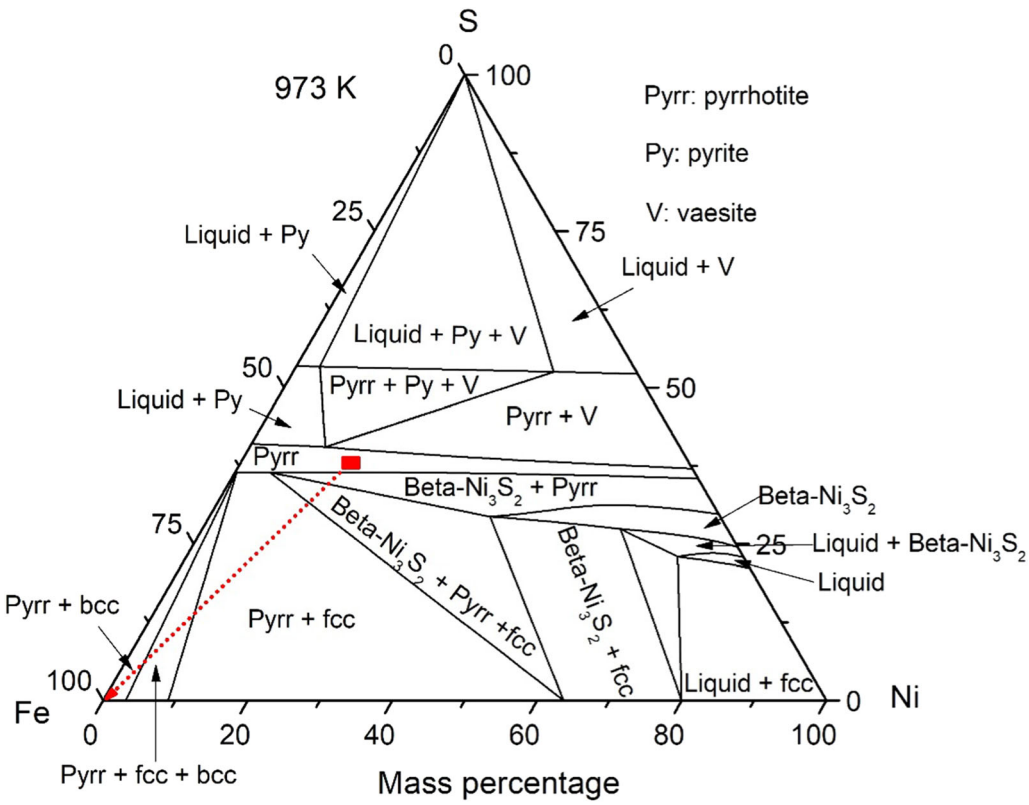

Fig. 2—Fe-Ni-S phase diagram at 973 K, calculated by FactSage™ 6.4.[18] The Pyrr is a Fe-deficient solid sulfide, and the liquid is a matte. Bcc and fcc are both FeNi alloy with different crystal structures. The solid square represents the initial concentrate composition.

C. *Chemical Composition*

The resulting sulfide phase after thermal treatment at different times was analyzed by electron microprobe, and the results are listed in Table III. As time increases, Ni concentration in the sulfide is reduced from 25.2 mass pct to 0.4 mass pct, demonstrating a process of Ni depletion. The stoichiometry of the resulting sulfide is close to the FeS phase.

Table IV shows the Ni concentration in the two types of FeNi particles; as seen, Ni content of the alloys ranges widely. Therefore, an arithmetic average of Ni content is not the best representative of the grade, hence the presented proportions based on the population.

D. *Release of S*

In the experiments, when transferring the samples between the hot and the cold zone, a small oxygen ingress is inevitable. As a result, a small amount of SO_2 was expected. The O_2 and SO_2 concentrations of the off gas were analyzed with respect to time, and thereby the cumulative volumes of the evolved SO_2 against time together with the mass pct of released S were calculated (Figure 7).

As seen, the amount of S lost into the off gas as SO_2 increases with time; but the overall amount is small. In 360 minutes, approximately 69 mL of SO_2 was evolved, representing ~ 0.7 mass pct of the bulk S of the concentrate. Hence the proposed process will

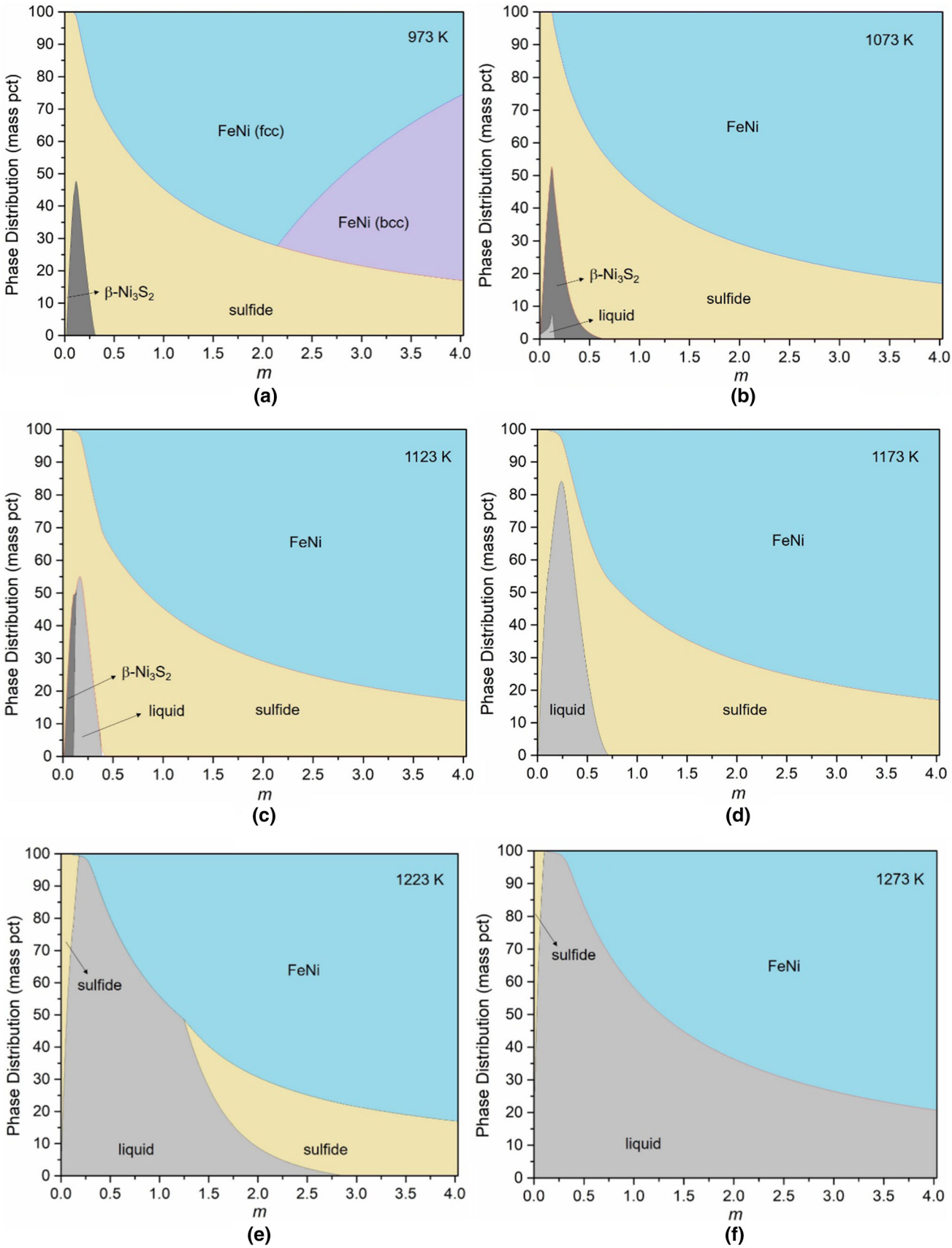

Fig. 3—Phase constitutions in the concentrate-Fe system as a function of temperature and mass ratio of Fe addition to Ni concentrate (*m*): (*a*) 973 K, (*b*) 1073 K, (*c*) 1123 K, (*d*) 1173 K, (*e*) 1223 K, and (*f*) 1273 K.

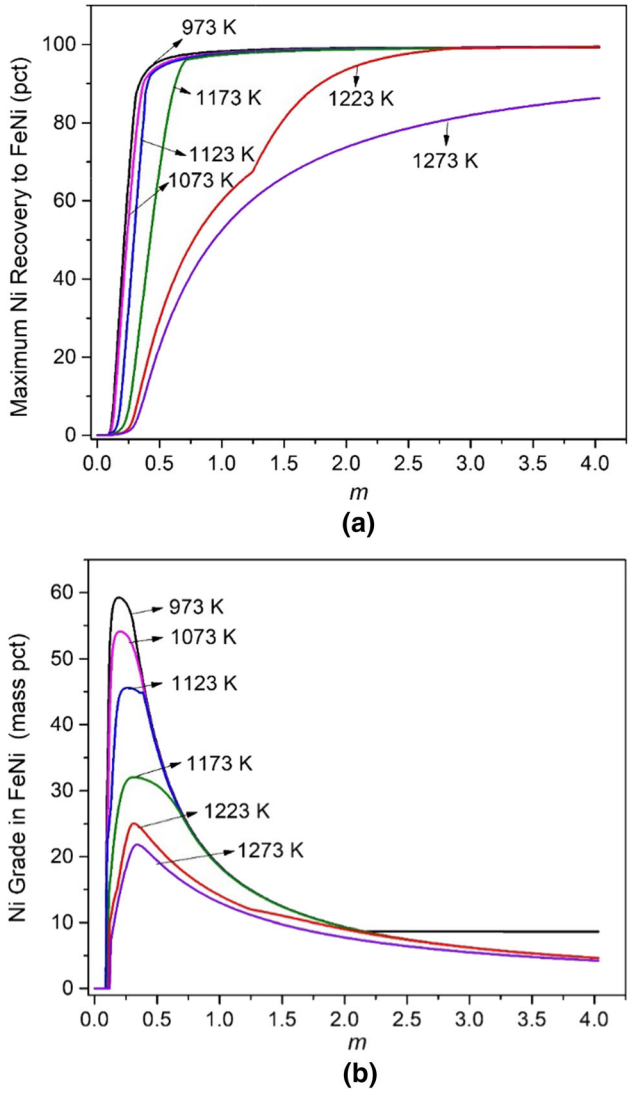

Fig. 4—Effect of Fe addition and temperature on theoretical Ni recovery to FeNi (*a*) and Ni grade in FeNi (*b*). *m* is the mass ratio of Fe addition to Ni sulfide concentrate.

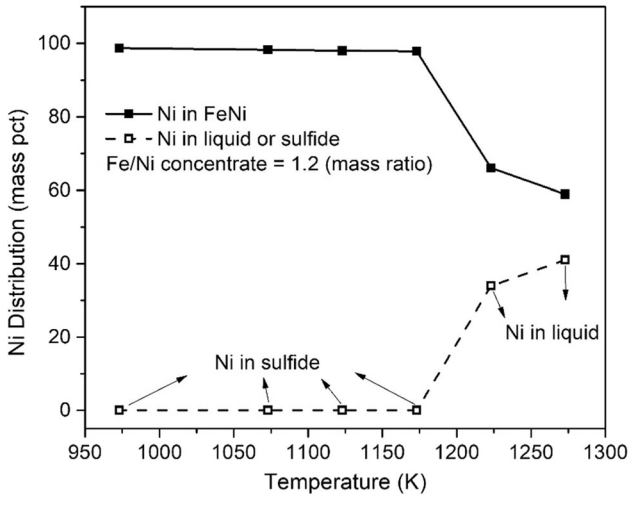

Fig. 5—Ni distribution in FeNi, solid sulfide, and liquid against temperature at $m = 1.2$.

significantly contribute to the mitigation of SO_2 emission. Furthermore, due to the decomposition of sulfide in the sample at 1073 K, a small amount of S is likely to be released as S_2 vapor into the off gas.

E. *Ni Grade and Recovery*

The recovery of Ni to the FeNi and the average Ni content were quantified by two methods. In the first method, image analysis on several regions of the sample in combination with the analysis of residual Ni in the sulfide phase and total Ni content of the sample was employed in a mass balance equation. The results are presented as a function of the total area of sample analyzed, as shown in Figure 8. At 10 minutes, the heat treatment generates a FeNi with ~ 18 mass pct Ni, and approximately 89 pct of the total Ni is extracted to the FeNi. The mass pct of alloy (FeNi) in the FeNi-sulfide system is 51 pct. At 30 minutes, the Ni recovery is increased to 97 pct, suggesting a near complete extraction. Further treatment beyond 30 minutes appears unnecessary.

In the second method, microprobe point analysis of the phases in the product together with mass balance, yielded the same parameters as the image analysis method. Note that the majority of S is retained in the solid FeS with ~ 0.7 mass pct of S reporting to the off gas as SO_2 (Figure 7(b)); furthermore, the FeNi contains ~ 0.03 mass pct S. A mass balance on Fe, Ni, and S under these conditions yielded the results in Table V. At 30 minutes, the maximum recovery reaches 98 pct, and the average Ni grade is 16 mass pct. Further increase in time does not improve the recovery and grade significantly. The results of the two methods are well consistent.

Figure 9 compares the experimentally determined Ni grade, FeNi mass percentage, and Ni recovery with the values predicted by thermodynamic evaluations. The experimental and theoretical values are in good agreement with each other for reaction times of 30 minutes or longer, indicating that the equilibrium has been reached, and that thermodynamic evaluation is adequate to assess the effects of processing temperature and the amount of Fe addition on Ni extraction from the sulfide.

F. *FeNi Particle Size*

Particle size is a significant parameter that affects the liberation and separation of FeNi from the host sulfides. Image analysis was employed to estimate the FeNi particle size before separation.[21,22] The particle size distribution for different treatment times is plotted in Figure 10(a).

As seen, in a relatively wide range of 5 to 360 minutes, treatment time has a small effect on the particle size, with ~ 70 mass pct of the particles in the 14 to 45 μm range, and no particle being larger than 80 μm. Intensive grinding is necessary to liberate such small FeNi particles from the sulfides. According to Wills and Finch,[23] to obtain a 75 pct degree of liberation, the ground sulfide particle size should be less than 4.5 μm, 10 times smaller than the FeNi particle size, *i.e.*, d_{80} =

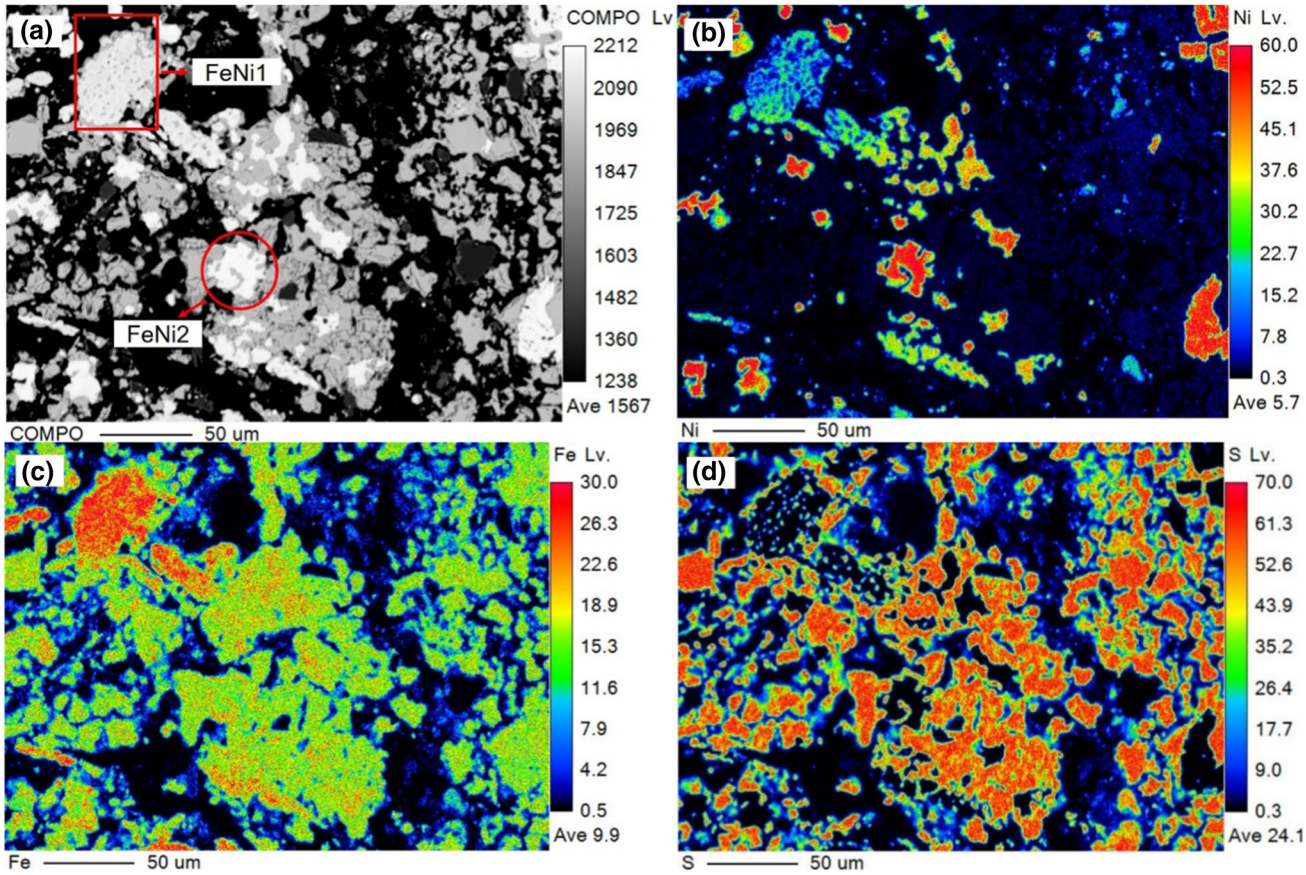

Fig. 6—BSE image of the thermal treatment products heated at 1073 K for 240 minutes (*a*) and EPMA mapping of Ni (*b*), Fe (*c*), and S (*d*) in the products.

Table III. Chemical Composition Analysis of Sulfide by EPMA

		Composition (Mass Pct)				
Phase	Time (Minutes)	Ni	Fe	S	Fe/S (Molar Ratio)	Measurements
Sulfide	5	25.2 ± 2.7	40.0 ± 1.7	31.6 ± 2	0.73	12
	10	1.4 ± 0.9	60.3 ± 1.1	35.9 ± 0.2	0.96	11
	30	0.5 ± 0.2	61.3 ± 0.9	36.8 ± 0.5	0.96	13
	60	0.4 ± 0.05	62.1 ± 0.7	36.7 ± 0.3	0.97	22
	120	0.4 ± 0.07	62.1 ± 0.4	36.7 ± 0.5	0.97	18
	240	0.6 ± 0.02	61.8 ± 0.5	36.3 ± 0.3	0.98	11
	360	0.4 ± 0.05	61.9 ± 0.5	36.7 ± 0.4	0.97	13

Table IV. Chemical Composition Analysis of FeNi by EPMA

Type of FeNi	Ni Grade (Mass Pct)	Proportion (Pct)	Total Measurements
FeNi1	< 5	73	15
	5 – 17	27	
FeNi2	< 20	17	24
	20 – 60	83	

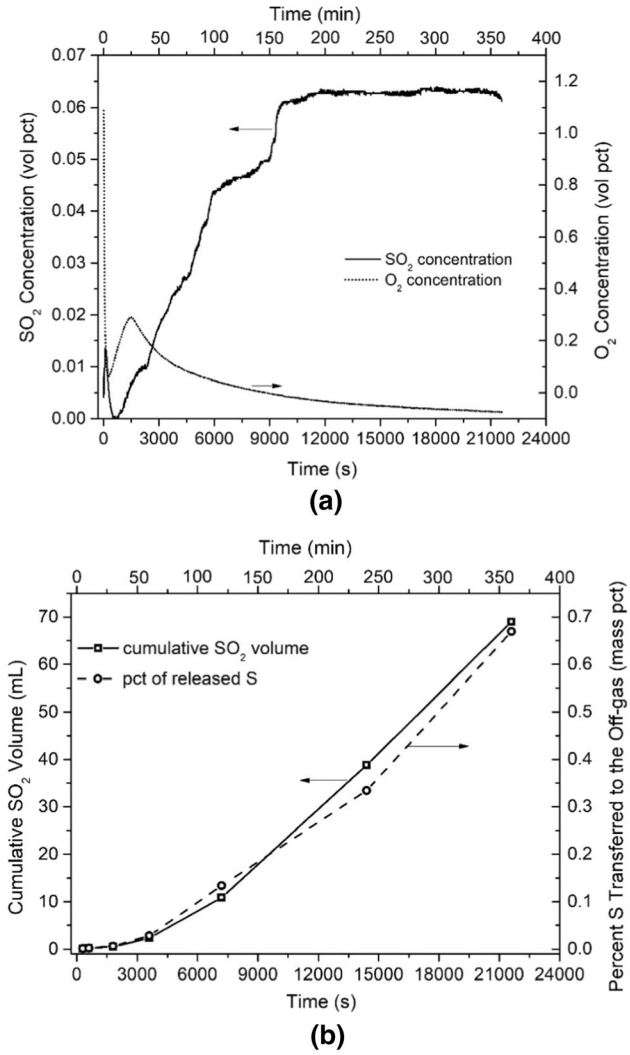

Fig. 7—(*a*) SO_2 and O_2 concentrations in the off gas at the different heating time; (*b*) the cumulative SO_2 volumes and the percent of S of the concentrate released as SO_2 to the off gas. The gas flow rate is 400 mL/minutes, and the temperature is 1073 K.

45 μm. Achieving this particle size is a challenge for any comminution process. Efforts are now underway to promote the FeNi particle size to a recoverable level by a variety of methods.

An interesting observation here is that the size of the FeNi particles is smaller than the size of the added metallic Fe. This can be associated with two reasons. First, some very small FeNi particles are precipitated in the sulfide matrix (Figure 10(b)) and separate from the original Fe particles; they reduce the cumulative size distribution. Their effect is, however, small as they do not constitute a large mass fraction of the sample. Another reason is the sulfidation of metallic Fe by the S which is unlocked during Ni migration.[14]

Based on the influence of the heating time on Ni grade, recovery, and FeNi particle size, the minimum heating time for solid-state extraction of Ni at 1073 K is selected as 30 min. Under these conditions, a FeNi alloy with approximately 16 to 18 mass pct Ni, the maximum recovery of ~ 97 pct, and a particle size of d_{80}(FeNi) = 45 μm were achieved.

G. *Mineralogical Changes*

Figure 11 compares the XRD patterns of the concentrate and the thermal treatment products. The original concentrate is mainly composed of pentlandite, pyrrhotite, pyrite, chalcopyrite, and silica. Ni is primarily present in pentlandite. By the end of the process, however, Ni exists in the two FeNi alloys nominally labeled as $Fe_{0.95}Ni_{0.05}$ and $Fe_{0.71}Ni_{0.29}$. Silica (gangue) remains essentially neutral in the process.

IV. CONCLUSIONS

This work investigated the minimum treatment time required for the solid-state extraction of Ni from sulfide concentrates. The experimental conditions were decided by a thermodynamic evaluation. The following conclusions were drawn.

(1) Solid-state extraction of Ni from Ni sulfide concentrate as FeNi alloy is feasible.
(2) At 973 K to 1173 K, the maximum Ni recovery to FeNi and Ni grade in FeNi are higher than those obtained at 1223 K to 1273 K. With increasing Fe addition, the recovery is increased, but the grade is decreased.
(3) Considering the thermodynamic evaluation, suitable operating conditions in terms of temperature and Fe: concentrate ratio are T = 973 K to 1173 K, and m = 0.5 to 2, respectively. Under these conditions, the maximum theoretical Ni recovery to FeNi and Ni grade are 94 to 98 pct and 10 to 36 mass pct, respectively.
(4) A minimum processing time of 30 minutes is required for m = 1.2 and T = 1073 K. Under these

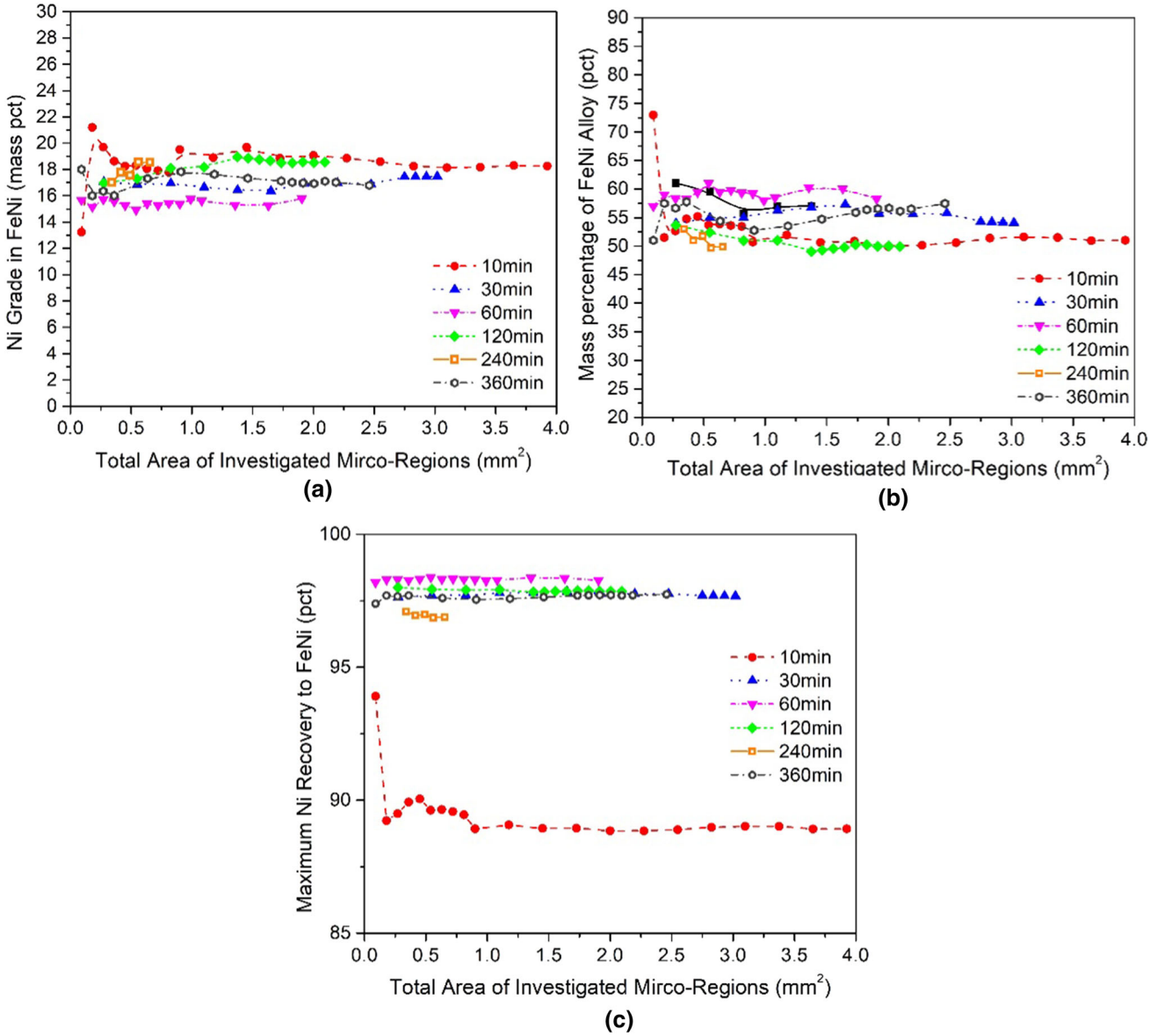

Fig. 8—(*a*) Average Ni grade in all FeNi, (*b*) mass percentage of all FeNi in the FeNi-sulfide system, and (*c*) maximum Ni recovery to FeNi.

Table V. Results Derived by EPMA Point Analysis and Mass Balance

Heating Time (Minutes)	Ni Grade in FeNi (Mass Pct)	Maximum Ni Recovery to FeNi (Pct)	Mass Percentage of FeNi (Mass Pct)
10	15	93	54
30	16	98	59
60	16	98	59
120	16	98	59
240	16	97	59
360	16	98	59

conditions, the residual Ni concentration in the resulting sulfide is 0.5 ± 0.2 mass pct; the Ni grade in FeNi is 16 to 18 mass pct; and the maximum Ni recovery to FeNi is ~ 97 pct. These experimental results are in agreement with the thermodynamic evaluations.

(5) During the 360 minutes of the thermal treatment, ~ 0.7 mass pct of the total S content in the concentrate was detected to be released as SO_2.

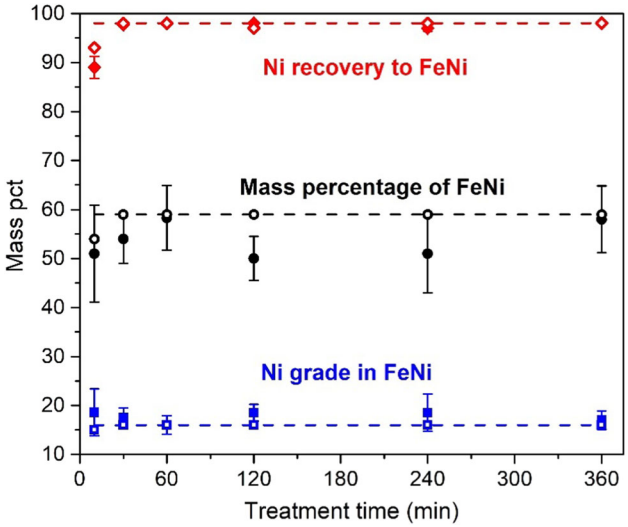

Fig. 9—Experimentally determined indicators and thermodynamic assessments. The solid symbols with error bars (standard deviations) are the image analysis results; the hollow symbols are the mass balance results; the dashed lines are theoretical predictions.

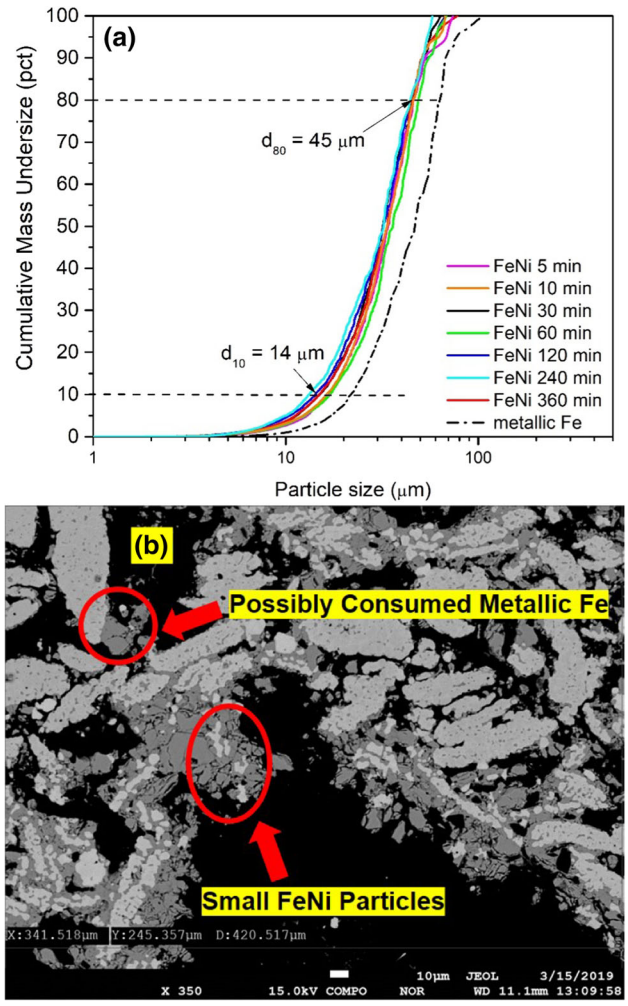

Fig. 10—(*a*) Size distribution of FeNi particles at various heating time and (*b*) BSE image of thermal treatment products. T = 1073 K, m = 1.2, and d_{100}(Fe) = 74 μm.

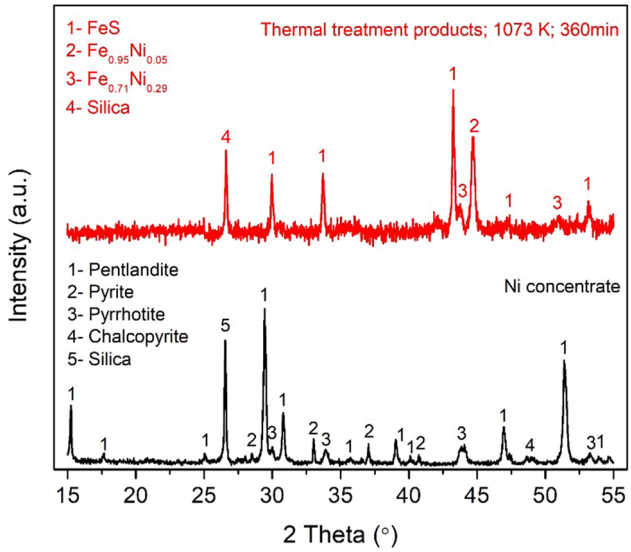

Fig. 11—XRD patterns of samples before and after thermal treatment.

(6) Most FeNi particles are distributed in 14 to 45 μm. Increasing time is inefficient in enhancing the particle size at 1073 K.

ACKNOWLEDGMENTS

The authors wish to acknowledge the financial support from the Natural Science and Engineering Research Council of Canada (NSERC, STPGP 479533-15), Process Research Ortech Inc., and technical support from XPS Consulting & Testwork Services, Glencore and Vale Canada. Fanmao Wang was partially supported by the China Scholarship Council (CSC, No. 201708530245). Sincere thanks to Dr. Abdolkarim Danaei for his help with the experiments. Mr. Richard Elliott and Mr. Feng Liu also provide insightful discussions for this research.

REFERENCE

1. A. Bautista, G. Blanco, and F. Velasco: *Cem. Concr. Res.*, 2006, vol. 36, pp. 1922–30.
2. D. Ryoo, N. Kang, and C. Kang: *Mater. Sci. Eng. A*, 2011, vol. 528, pp. 2277–81.
3. L.N. Zhang and O.A. Ojo: *Metall. Mater. Trans. A*, 2018, vol. 49, pp. 295–304.
4. C. Chakkaravarthy, P. Periasamy, S. Jegannathan, and K.I. Vasu: *J. Power Sources*, 1991, vol. 35, pp. 21–35.
5. F.K. Crundwell, M.S. Moats, V. Ramachandran, T.G. Robinson, and W.G. Davenport: *Extractive Metallurgy of Nickel, Cobalt and Platinum Group Metals*, Elsevier, New York, 2011, pp. 21–37.
6. D.Q. Zhu, Y. Cui, K. Vining, S. Hapugoda, J. Douglas, J. Pan, and G.L. Zheng: *Int. J. Miner. Process.*, 2012, vols. 106–109, pp. 1–7.
7. F.K. Crundwell, M.S. Moats, V. Ramachandran, T.G. Robinson, and W.G. Davenport: *Extractive Metallurgy of Nickel,* Cobalt and Platinum Group Metals, Elsevier, New York, 2011, pp. 247–57.
8. G. Li, H. Cheng, S. Chen, X. Lu, Q. Xu, and C. Lu: *Metall. Mater. Trans. B*, 2018, vol. 49, pp. 1136–48.

9. W. Mu, F. Cui, H. Xin, Y. Zhai, and Q. Xu: *Hydrometallurgy*, 2020, vol. 191, p. 105187.
10. W. Mu, F. Cui, Z. Huang, Y. Zhai, Q. Xu, and S. Luo: *J. Clean. Prod.*, 2018, vol. 177, pp. 371–77.
11. D. Yu, T.A. Utigard, and M. Barati: *Metall. Mater. Trans. B*, 2014, vol. 45B, pp. 653–61.
12. D. Yu, T.A. Utigard, and M. Barati: *Metall. Mater. Trans. B*, 2014, vol. 45B, pp. 662–74.
13. R. Sridhar, A. Dalvi, H.F. Bakker, and A. Illis: *Can. Metall. Q.*, 1976, vol. 15, pp. 255–62.
14. F. Liu, D. Yu, S. Marcuson, F. Wang, B. Li, and M. Barati: *Miner. Eng.*, 2019, vol. 134, pp. 206–14.
15. D. Yu, F. Liu, J. Zhang, and M. Barati: *Metall. Mater. Trans. B*, 2019, vol. 50, pp. 2186–96.
16. F. Wang, F. Liu, R. Elliott, S. Rezaei, L.T. Khajavi, and M. Barati: *J. Alloys Compd.*, 2020, vol. 822, p. 153582.
17. H.M. Cobb: *Steel Products Manual: Stainless Steels*, Warrendale, 1999.
18. C.W. Bale, E. Bélisle, P. Chartrand, S.A. Decterov, G. Eriksson, A.E. Gheribi, K. Hack, I. Jung, Y. Kang, J. Melançon, A.D. Pelton, S. Petersen, C. Robelin, J. Sangster, P. Spencer, and M. Van Ende: *Calphad*, 2016, vol. 54, pp. 35–53.
19. F.K. Crundwell, M.S. Moats, V. Ramachandran, T.G. Robinson, and W.G. Davenport: *Extractive Metallurgy of Nickel, Cobalt and Platinum Group Metals*, Elsevier, New York, 2011, pp. 49–53.
20. O. Polyakov: *Handbook of Ferroalloys Theory and Technology*, 12th ed., Elsevier, New York, 2013, pp. 367–75.
21. B.V. Miller and R.W. Limes: *Crit. Rev. Anal. Chem.*, 1988, vol. 20, pp. 75–116.
22. F.M. Etzler and R. Deanne: *Part. Part. Syst. Charact.*, 1997, vol. 14, pp. 278–82.
23. B. Wills and J. Finch: *Wills' Mineral Processing Technology*, 8th ed., Elsevier, New York, 2015, pp. 1–27.